# Permittivity of a multiphase and isotropic lattice of spheres at low frequency

Keith W. Whites[a)]
*Department of Electrical Engineering, University of Kentucky, 453 Anderson Hall, Lexington, Kentucky 40506-0046*

(Received 30 September 1999; accepted for publication 10 May 2000)

A solution methodology is presented in this article to compute the effective permittivity for a multiphase lattice of dielectric and/or conducting spheres at low frequencies. It is assumed that the lattice is effectively isotropic. This methodology relies on two central developments. The first is a *T*-matrix solution for a multiphase lattice of spheres immersed in a uniform electric field. This solution is presented in a succinct matrix-vector notation and is valid for any lattice type. The second development is a simple and accurate equation for the effective permittivity that incorporates all mutual coupling between the spheres. Results are shown in this article for three situations. The first is a two-phase system of conducting spheres (used for verification) and the second is a dielectric-conductor (cermet composite) lattice of spheres. The third and final result is from a lattice containing a *cluster* of conducting spheres. It is suggested that this last material type displays a behavior in between that of random materials and two-phase lattices due to ''permittivity enhancement'' at low volume fraction. It is also shown that the Maxwell Garnett formula is not nearly as accurate for this cluster lattice, also because of this enhancement effect. © *2000 American Institute of Physics.* [S0021-8979(00)02116-2]

## I. INTRODUCTION AND OVERVIEW

Effective media models can provide dramatic simplification to problems involving large numbers of electromagnetically small particles collected in space. Rather than compute the scattering by each particle individually, the effective macroscopic material parameters can be used with the constitutive relations to simplify the analysis. The purpose of effective media modeling is to obtain accurate values for these macroscopic material parameters. Provided the scattering by the particles is computed accurately (including mutual coupling) and a proper constitutive model is chosen, then effective media theory can provide incredible computational simplification to these types of problems. In reality, this may be the only way to render the problem tractable.

Of course, effective media computation is not a new topic of research. In his treatise, Maxwell provided a simple derivation of the effective conductivity (resistivity) for a collection of weakly interacting spheres in a conductive (resistive) space.[1] In an analogous manner, the effective permittivity $\varepsilon_{r,\text{eff}}$ for a collection of weakly interacting dielectric spheres of relative permittivity $\varepsilon_r$ and volume fraction $f$ can be obtained from Maxwell's work as

$$\varepsilon_{r,\text{eff}} = 1 + 3\frac{f(\varepsilon_r - 1)/(\varepsilon_r + 2)}{1 - f(\varepsilon_r - 1)/(\varepsilon_r + 2)}, \tag{1}$$

since both problems are governed by Laplace's equation. Equation (1) is commonly called the Maxwell Garnett (MG) equation[2–4] but was derived by Maxwell some 30 years previous.

This famous and ''remarkable''[5] equation provides extremely good predictions of low frequency effective media parameters for spherical particles with only weak mutual interaction. Rayleigh was the first to more accurately compute the effective permittivity (conductivity) for a mixture of particles.[5,6] He considered a simple cubic lattice of spheres allowing for dipole and octupole interactions. McPhedran and McKenzie[7,8] greatly extended Lord Rayleigh's method and included arbitrarily high multipole interactions between spheres making the technique ''numerically exact'' for all three cubic lattice types.

Accurate experimental measurements for the effective conductivity of cubic lattices of spheres have also been presented in the literature. Kharadly and Jackson[9] and Meredith and Tobias[10] presented effective conductivity measurements for simple cubic lattices of perfectly conducting spheres. Similar measurements for the effective conductivity of body-centered-cubic lattices of perfectly conducting spheres were obtained by McKenzie *et al.*[8]

Two-phase materials (host plus spheres) were the only systems considered in all of the analyses and experimental measurements mentioned above. The main purpose of this article is to present a method to compute the effective permittivity for a multiphase system of dielectric and/or conducting spheres in a lattice, that is, lattices comprised of unit cells containing many spheres of different size and/or composition.

Multiphase materials are more accurate representations for many realistic composites.[11] For example, when small inclusions are manufactured from a large sample by a grinding technique, a wide range of particle sizes often results. Conversely, other multiphase systems are just naturally combinations of different material types. Examples of this in-

a)Electronic mail: whites@engr.uky.edu

 © 2000 American Institute of Physics

clude effective media models for soil which contain solid particles, water and background;[12] wet snow which contain ice, water and background;[3] and seed kernels which contain grain, water and background.[13]

These multiphase material examples all represent random collection of particles. The emphasis of this article, however, is on ordered arrangement of particles. Like random media, multiphase lattice theory also has many practical applications. Multicomponent crystals are such an example where multiphase lattice theory is necessary.[14] There are also examples in the literature involving photonic crystals where effective media representation is applicable, primarily through the concept of homogenization.[15,16]

In this article, we present a scattering solution for a multiphase lattice of dielectric and/or conducting spheres in a uniform and time-stationary electric field. This *T*-matrix solution is presented in the efficient matrix-vector notation of Chew.[17] A simple algorithm for the computation of the effective permittivity $\varepsilon_{r,\text{eff}}$ of this multiphase system is also given. It is assumed in this work that the lattice possesses sufficient symmetry to yield isotropic macroscopic material parameters. In the case of a two-phase system, the development of this equation for $\varepsilon_{r,\text{eff}}$ is much more direct than that presented by previous researchers.[5,7,8]

Numerical $\varepsilon_{r,\text{eff}}$ results computed with our technique for three cases are shown towards the end of the article. The first is a verification of our multiphase lattice scattering equations and the subsequent computer codes used to numerically solve them. This verification is manifested through comparisons of numerical and experimental results for conducting spheres in a body-centered-cubic lattice.[8]

This is followed by two sets of multiphase lattice results. The first is a three-phase lattice containing both dielectric and conducting spheres. The second is a nine-phase system containing eight conducting spheres arranged in a cluster. Dielectric enhancement at low volume fraction is illustrated in this example and is circumstantial evidence for the effective cluster model of random mixtures put forth by Doyle and Jacobs.[18] This last set of data can also be used to support the concept of a new class of material, that is, a material with characteristics between those of lattices and random materials.

## II. *T*-MATRIX SOLUTION FOR POTENTIAL SCATTERING

As mentioned in Sec. I, the lattice of interest in this work is composed of unit cells with potentially many spheres as shown in Fig. 1. It will be required that each sphere remains charge neutral when illuminated by the incident electric field $\boldsymbol{E}^{\text{inc}}$, which will be assumed constant everywhere but orientated in an arbitrary direction. Furthermore, it will also be required that the lattice remains effectively isotropic.

In order to compute the effective permittivity $\varepsilon_{r,\text{eff}}$ of this multiphase lattice, we first need to compute the electric dipole moments $\boldsymbol{p}_i$ of each sphere $i=1,...,N$ located in a primitive unit cell. These electric dipole moments will be determined using a *T*-matrix solution that accurately computes the scalar potential scattering by the spheres and includes the effects of mutual interaction between them.

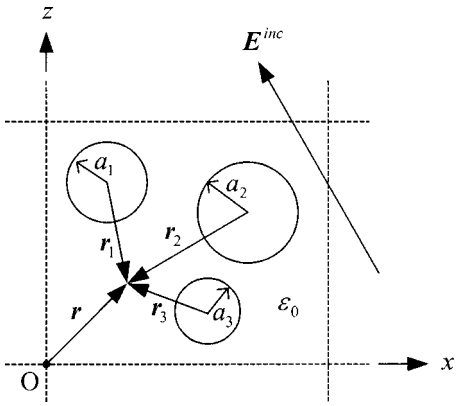


FIG. 1. Geometry of a prototypical unit cell in the infinite lattice of spheres illuminated by a uniform incident electric field $\mathbf{E}^{\text{inc}}$.

In terms of spherical harmonics the incident scalar potential field can be expressed in the coordinates of the global origin 0 as[17,19,20]

$$\phi^{\text{inc}}(\mathbf{r}_0)=\sum_{l=0}^{\infty}\sum_{m=-l}^{l} Y_l^m(\Omega_0) r_0^l u_{lm}. \tag{2}$$

In this expression, the spherical harmonic function is defined as

$$\begin{aligned} Y_l^m(\Omega_0) &= Y_l^m(\theta_0,\phi_0) \\ &= (-1)^m \sqrt{\frac{2l+1}{4\pi}\frac{(l-m)!}{(l+m)!}} P_l^m(\cos\theta_0) e^{-jm\phi_0}, \end{aligned} \tag{3}$$

where $P_l^m$ is the associated Lengendre polynomial defined according to Stratton[21] and $j$ is the imaginary unit. Using the matrix-vector notation of Chew,[17,19] Eq. (2) can be written in the compact form

$$\phi^{\text{inc}}(\mathbf{r}_0)=Rg\boldsymbol{\psi}^T(\mathbf{r}_0)\cdot\mathbf{u}, \tag{4}$$

where $Rg\boldsymbol{\psi}^T(\mathbf{r}_0)$ is a row vector containing the regular (nonsingular) function

$$Rg\boldsymbol{\psi}^T(\mathbf{r}_0)=\mathbf{Y}^T(\Omega_0)\cdot\overline{\mathbf{r}}_0 \tag{5}$$

in terms of coordinate system 0. In Eq. (4), $\mathbf{u}$ is a column vector containing the coefficients $u_{lm}$ of the incident scalar potential for a uniform electric field (see Table I) while in Eq. (5), $\mathbf{Y}^T(\Omega_0)$ is a row vector containing $Y_l^m(\theta_0,\phi_0)$ and $\overline{\mathbf{r}}_0$ is a diagonal matrix containing $r_0^l$.

The development of this *T*-matrix solution is highly dependent on the use of addition (translation) formulas which facilitate the expression of spherical harmonics of one spherical coordinate system in those of another.[17,19,22–24] The two addition formulas that will be used in this work are given in Eqs. (A1) and (A2) of the Appendix. Considering the $i$th sphere (of $N$) in the $j$th unit cell, the scattered potential produced by this sphere, numbered as $p=(j-1)N+i$, is

TABLE I. $\phi^{\text{inc}}$ spherical expansion coefficients, i.e., the $u_{lm}$ of Eq. (4), for uniform incident electric fields in the three Cartesian directions. The other coefficients ($l \neq 1$) are zero for all three expansions. ($j$ = imaginary unit.)

| | | $u_{lm}$ | | |
|---|---|---|---|---|
| $l$ | $m$ | for $\mathbf{E}^{\text{inc}} = \hat{\mathbf{x}} E_{x0}$ | for $\mathbf{E}^{\text{inc}} = \hat{\mathbf{y}} E_{y0}$ | for $\mathbf{E}^{\text{inc}} = \hat{\mathbf{z}} E_{z0}$ |
| 1 | $-1$ | $-E_{x0}\sqrt{\frac{2\pi}{3}}$ | $jE_{y0}\sqrt{\frac{2\pi}{3}}$ | 0 |
| 1 | 0 | 0 | 0 | $-E_{z0}\sqrt{\frac{4\pi}{3}}$ |
| 1 | 1 | $E_{x0}\sqrt{\frac{2\pi}{3}}$ | $jE_{y0}\sqrt{\frac{2\pi}{3}}$ | 0 |

$$\phi_p^{\text{scat}}(\mathbf{r}_p) = \phi_{i,j}^{\text{scat}}(\mathbf{r}_p) = \boldsymbol{\psi}^T(\mathbf{r}_p) \cdot \overline{\mathbf{T}}_{i,j} \cdot \hat{\bar{\boldsymbol{\beta}}}_{p0} \cdot \mathbf{u}. \tag{6}$$

The observation vector $\mathbf{r}_p$ is defined in the local spherical coordinate system of particle $p$ and is assumed to terminate at points external to all spheres. In Eq. (6), $\boldsymbol{\psi}^T(\mathbf{r}_p)$ is a row vector containing the singular function

$$\boldsymbol{\psi}^T(\mathbf{r}_p) = \mathbf{Y}^T(\Omega_p) \cdot (\overline{\mathbf{r}}_p r_p)^{-1}, \tag{7}$$

where $(\overline{\mathbf{r}}_p r_p)^{-1}$ is a diagonal matrix containing $r_p^{-(l+1)}$ and $\overline{\mathbf{T}}_{i,j}$ is the (dense) $T$ matrix of sphere $i$ within unit cell $j$ in the presence of all other spheres in the lattice. The matrix $\hat{\bar{\boldsymbol{\beta}}}_{p0}$ translates the spherical harmonic coefficients of the incident field from the coordinates of the global origin to the coordinates of sphere $p$.

The total scalar potential at any point $\mathbf{r}$ located exterior to all spheres in the lattice is the sum of the incident potential, Eq. (4), plus the scattered potential, Eq. (6), due to all spheres in the infinite lattice,

$$\phi(\mathbf{r}) = Rg\, \boldsymbol{\psi}^T(\mathbf{r}_0) \cdot \mathbf{u} + \sum_{j=1}^{\infty} \sum_{i=1}^{N} \boldsymbol{\psi}^T(\mathbf{r}_p) \cdot \overline{\mathbf{T}}_{i,j} \cdot \hat{\bar{\boldsymbol{\beta}}}_{p0} \cdot \mathbf{u}. \tag{8}$$

Because the lattice is infinite, each particle $i$ in lattice cell $j$ will have the same $T$ matrix. Therefore, we will choose

$$\overline{\mathbf{T}}_{i,j} = \overline{\mathbf{T}}_{i,1}, \quad i = 1,...,N. \tag{9}$$

Hence, substituting Eq. (9) into Eq. (8) gives

$$\phi(\mathbf{r}) = Rg\, \boldsymbol{\psi}^T(\mathbf{r}_0) \cdot \mathbf{u} + \sum_{j=1}^{\infty} \sum_{i=1}^{N} \boldsymbol{\psi}^T(\mathbf{r}_p) \cdot \overline{\mathbf{T}}_{i,1} \cdot \hat{\bar{\boldsymbol{\beta}}}_{p0} \cdot \mathbf{u}. \tag{10}$$

Without loss of generality, we will focus on particle $i'$ within unit cell 1. The scattered potential from particle $i' = 1,...,N$ will be removed from the summation in Eq. (10) to give

$$\phi(\mathbf{r}) = Rg\, \boldsymbol{\psi}^T(\mathbf{r}_{i'}) \cdot \hat{\bar{\boldsymbol{\beta}}}_{i'0} \cdot \mathbf{u} + \boldsymbol{\psi}^T(\mathbf{r}_{i'}) \cdot \overline{\mathbf{T}}_{i',1} \cdot \hat{\bar{\boldsymbol{\beta}}}_{i'0} \cdot \mathbf{u} + \sum_{j=1}^{\infty} {\sum_{i=1}^{N}}' Rg\, \boldsymbol{\psi}^T(\mathbf{r}_{i'}) \cdot \hat{\bar{\boldsymbol{\alpha}}}_{i'p} \cdot \overline{\mathbf{T}}_{i,1} \cdot \hat{\bar{\boldsymbol{\beta}}}_{p0} \cdot \mathbf{u}. \tag{11}$$

In this expression, the addition formulas (A1) and (A2) have been used to express the incident and scattered potentials in the local spherical coordinate system of particle $i'$. The prime on the summation indicates that the term $i = i'$, $j = 1$ is to be excluded from the sum since in this case $p = i'$.

Equation (11) can be simplified by taking advantage of the fact that the particles are assumed charge neutral and located in a uniform incident electric field. Because of this, each similarly located particle within a unit cell will be identically polarized. Consequently, the scattered potential produced by similarly located particles within two different unit cells will be identically equal at the same relative locations with respect to the centroids of these two particles. That is, from Eq. (6) for two similarly located spheres $i$ in two different unit cells $s$ and $t$,

$$\phi_{i,s}^{\text{scat}}(\mathbf{v}) = \phi_{i,t}^{\text{scat}}(\mathbf{v}), \tag{12}$$

so that with Eq. (9)

$$\boldsymbol{\psi}^T(\mathbf{v}) \cdot \overline{\mathbf{T}}_{i,1} \cdot \hat{\bar{\boldsymbol{\beta}}}_{(s-1)N+i,0} \cdot \mathbf{u} = \boldsymbol{\psi}^T(\mathbf{v}) \cdot \overline{\mathbf{T}}_{i,1} \cdot \hat{\bar{\boldsymbol{\beta}}}_{(t-1)N+i,0} \cdot \mathbf{u}, \tag{13}$$

where $\mathbf{v}$ is some arbitrary vector that places the observation point external to the particles. Provided $\overline{\mathbf{T}}_{i,1}^{-1}$ exists, which is assumed throughout this work, then it can be deduced from Eq. (12) that

$$\hat{\bar{\boldsymbol{\beta}}}_{p0} \cdot \mathbf{u} = \mathbf{u} \quad \forall p. \tag{14}$$

Using this result in Eq. (11) gives

$$\phi(\mathbf{r}) = Rg\, \boldsymbol{\psi}^T(\mathbf{r}_{i'}) \cdot \mathbf{u} + \boldsymbol{\psi}^T(\mathbf{r}_{i'}) \cdot \overline{\mathbf{T}}_{i',1} \cdot \mathbf{u} + \sum_{j=1}^{\infty} {\sum_{i=1}^{N}}' Rg\, \boldsymbol{\psi}^T(\mathbf{r}_{i'}) \cdot \hat{\bar{\boldsymbol{\alpha}}}_{i'p} \cdot \overline{\mathbf{T}}_{i,1} \cdot \mathbf{u}. \tag{15}$$

Following the reasoning of Chew,[17,19] we can treat the first and third terms in Eq. (15) as the ''incident'' potential on sphere $i'$ when all other particles are removed. Consequently, the scattered potential spherical harmonics can be related to those of the ''incident'' potential through the isolated $T$ matrix of particle $i'$, $\overline{\mathbf{T}}_{i'(1)}$, as

$$\overline{\mathbf{T}}_{i',1} = \overline{\mathbf{T}}_{i'(1)} \cdot \left[ \overline{\mathbf{I}} + \sum_{j=1}^{\infty} {\sum_{i=1}^{N}}' \hat{\bar{\boldsymbol{\alpha}}}_{i'p} \cdot \overline{\mathbf{T}}_{i,1} \right] = \overline{\mathbf{T}}_{i'(1)} + \overline{\mathbf{T}}_{i'(1)} \cdot \sum_{j=1}^{\infty} {\sum_{i=1}^{N}}' \hat{\bar{\boldsymbol{\alpha}}}_{i'p} \cdot \overline{\mathbf{T}}_{i,1}. \tag{16}$$

This identity can be used to solve for $\overline{\mathbf{T}}_{i(1)}$ by interchanging sums and rearranging to yield

$$\overline{\mathbf{T}}_{i',1} - \overline{\mathbf{T}}_{i'(1)} \cdot \sum_{i=1}^{N} \left[ {\sum_{j=1}^{\infty}}' \hat{\bar{\boldsymbol{\alpha}}}_{i'p} \right] \cdot \overline{\mathbf{T}}_{i,1} = \overline{\mathbf{T}}_{i'(1)}. \tag{17}$$

This equation can be more explicitly written in matrix form by allowing $i'$ and $i$ to vary from 1 to $N$ for the rows and columns, respectively, of the matrix

$$\begin{bmatrix} \overline{\mathbf{I}}-\overline{\mathbf{T}}_{1(1)}\cdot\sum_{j=1}^{\infty}{}'\,\hat{\hat{\boldsymbol{\alpha}}}_{1,(j-1)N+1} & -\overline{\mathbf{T}}_{1(1)}\cdot\sum_{j=1}^{\infty}\hat{\hat{\boldsymbol{\alpha}}}_{1,(j-1)N+2} & \cdots & -\overline{\mathbf{T}}_{1(1)}\cdot\sum_{j=1}^{\infty}\hat{\hat{\boldsymbol{\alpha}}}_{1,(j-1)N+N} \\ -\overline{\mathbf{T}}_{2(1)}\cdot\sum_{j=1}^{\infty}\hat{\hat{\boldsymbol{\alpha}}}_{2,(j-1)N+1} & \overline{\mathbf{I}}-\overline{\mathbf{T}}_{2(1)}\cdot\sum_{j=1}^{\infty}{}'\,\hat{\hat{\boldsymbol{\alpha}}}_{2,(j-1)N+2} & & \vdots \\ \vdots & & \ddots & \\ -\overline{\mathbf{T}}_{N(1)}\cdot\sum_{j=1}^{\infty}\hat{\hat{\boldsymbol{\alpha}}}_{N,(j-1)N+1} & \cdots & & \overline{\mathbf{I}}-\overline{\mathbf{T}}_{N(1)}\cdot\sum_{j=1}^{\infty}{}'\,\hat{\hat{\boldsymbol{\alpha}}}_{N,(j-1)N+N} \end{bmatrix} \begin{bmatrix} \overline{\mathbf{T}}_{1,1} \\ \overline{\mathbf{T}}_{2,1} \\ \vdots \\ \overline{\mathbf{T}}_{N,1} \end{bmatrix} = \begin{bmatrix} \overline{\mathbf{T}}_{1(1)} \\ \overline{\mathbf{T}}_{2(1)} \\ \vdots \\ \overline{\mathbf{T}}_{N(1)} \end{bmatrix}. \tag{18}$$

A couple of points concerning the solution to Eq. (18) are relevant here. First, if a total of $L$ harmonics is used to expand the scattered potential of each particle (and the translation matrices $\hat{\hat{\boldsymbol{\alpha}}}$) and there are $N$ particles per unit cell, then the size of the dense matrix equation will be $LN$. Presumably, $N$ will be relatively small so this matrix equation is generally small, i.e., on the order of a few hundred unknowns.

Second, the elements of the right-hand side vector in Eq. (18) are the isolated $T$ matrices of all the spheres in the primitive unit cell. For static (time-invariant) illumination, these $T$ matrices will be those either for dielectric or for conducting spheres. These isolated $T$ matrices will be strictly diagonal and can be derived in a straightforward manner by enforcing appropriate boundary conditions between the incident, scattered and interior spherical harmonics. For a dielectric sphere with relative permittivity $\varepsilon_r$ and radius $a$ the elements of the isolated $T$ matrix are[19]

$$T_{lm,l'm'}=\frac{l(1-\varepsilon_r)}{1+l(1+\varepsilon_r)}a^{2l+1}\delta_{lm,l'm'}. \tag{19}$$

In the case of an ungrounded conducting sphere of radius $a$, the isolated $T$ matrix is

$$T_{lm,l'm'}=\begin{cases} 0 & l=0 \\ -a^{2l+1}\delta_{lm,l'm'} & l\neq 0 \end{cases}. \tag{20}$$

## III. EFFECTIVE PERMITTIVITY CALCULATION

The first step in computing the effective permittivity of this multiphase lattice is to choose an appropriate macroscopic model. The model to be applied here is that of a dielectric sphere of arbitrary radius and relative permittivity $\varepsilon_{r,\text{eff}}$ immersed in a uniform electric field as shown in Fig. 2. Without loss of generality, we will chose the incident field

$$\mathbf{E}_0=\hat{z}E_z^{\text{inc}} \tag{21}$$

to illuminate both this macroscopic sphere in Fig. 2 as well as the infinite lattice. Following Jackson,[20] the polarization density induced inside the sphere is

$$\mathbf{P}=(\varepsilon_{\text{eff}}-\varepsilon_0)\mathbf{E}=3\varepsilon_0\frac{\varepsilon_{r,\text{eff}}-1}{\varepsilon_{r,\text{eff}}+2}\mathbf{E}_0. \tag{22}$$

It will be assumed that the multiphase lattice contains sufficient symmetry to ensure isotropy for the permittivity.

The volume integral of $\mathbf{P}$ in Eq. (22) per unit cell (with volume $V_c$) can be considered equivalent to the vector sum of the dipole moments of all $N$ particles in the unit cell. That is, for this effectively isotropic multiphase system of particles immersed in the incident field Eq. (21),

$$\mathbf{P}=\hat{z}P_z=\hat{z}\sum_{i=1}^{N}\frac{p_{z,i}}{V_c}. \tag{23}$$

Substituting Eq. (23) into Eq. (22) gives

$$\sum_{i=1}^{N}\frac{p_{z,i}}{V_c}=3\varepsilon_0\frac{\varepsilon_{r,\text{eff}}-1}{\varepsilon_{r,\text{eff}}+2}E_z^{\text{inc}}. \tag{24}$$

Solving this equation yields

$$\varepsilon_{r,\text{eff}}=1+3\,\frac{1\Sigma_{i=1}^{N}p_{z,i}/(3\varepsilon_0E_z^{\text{inc}}V_c)}{1-1\Sigma_{i=1}^{N}p_{z,i}/(3\varepsilon_0E_z^{\text{inc}}V_c)}. \tag{25}$$

Once the electric dipole moments $p_{z,i}$ have been computed for each of the spheres in the primitive unit cell, this simple equation can then be used to compute the effective permittivity of the multiphase lattice.

Of course, the accuracy to which the dipole moments have been computed determines the accuracy of the effective permittivity. Namely, using the dipole moments computed from the $T$ matrix solution of the previous section will yield $\varepsilon_{r,\text{eff}}$ values from Eq. (25) that are ''numerically exact.'' Conversely, with $p_{z,i}$ determined under the approximation that there is no interaction between spheres yields the Maxwell Garnett formula. These two diametrically opposed situations are discussed below.

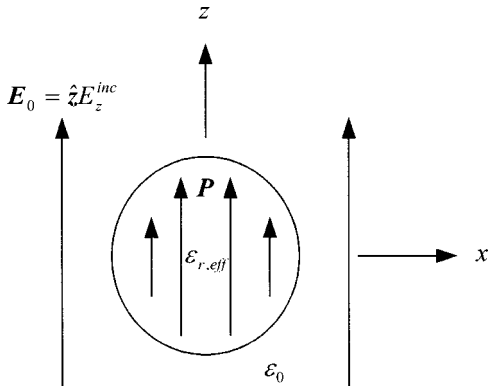


FIG. 2. Macroscopic sphere of effective permittivity $\varepsilon_{r,\text{eff}}$ illuminated by a uniform incident electric field $\mathbf{E}_0$.

### A. Computation of $p_{z,i}$ and $\varepsilon_{r,\text{eff}}$ from the *T*-matrix solution

The electric dipole moments $\mathbf{p}_i$ can be numerically determined from the *T*-matrix solution in Sec. II and the illumination specified in Eq. (21). The scattered potential produced by the $i$th sphere in unit cell $j=1$ is found from Eqs. (6) and (7) to be

$$\phi_i^{\text{scat}}(\mathbf{r}_i) = \boldsymbol{\psi}^T(\mathbf{r}_i)\cdot\overline{\mathbf{T}}_{i,1}\cdot\hat{\bar{\boldsymbol{\beta}}}_{i0}\cdot\mathbf{u} = \sum_{l=1}^{\infty}\sum_{m=-l}^{l} Y_l^m(\Omega_i) r_i^{-(l+1)} b_{lm}. \tag{26}$$

To determine $\mathbf{p}_i$, only the three $l=1$ terms in this potential are of importance since the potential produced by a point electric dipole varies as $r_i^2$. Using the results of Jackson[20] the $z$-directed electric dipole moment is found to be

$$p_{z,i} = \varepsilon_0\sqrt{12\pi}\,b_{10}. \tag{27}$$

The term $b_{10}$ denotes that only the row corresponding to the local spherical harmonic $l=1$, $m=0$ is to be used from the vector $\overline{\mathbf{T}}_{i,1}\cdot\hat{\bar{\boldsymbol{\beta}}}_{i0}\cdot\mathbf{u}$ in Eq. (26). This $p_{z,i}$ is then used in Eq. (25) for the computation of $\varepsilon_{r,\text{eff}}$.

### B. Computation of $p_{z,i}$ and $\varepsilon_{r,\text{eff}}$ without mutual coupling

An *approximate* expression for the effective permittivity can be derived quite easily if it is assumed that the electric dipole moment of the sphere is not influenced by other spheres in the lattice. When an isolated sphere is subjected to a uniform incident electric field as in Eq. (21), the induced electric dipole moment[20] is

$$p_{z,i} = 4\pi\varepsilon_0\frac{\varepsilon_{r,i}-1}{\varepsilon_{r,i}+2}a_i^3 E_z^{\text{inc}}, \tag{28}$$

where $a_i$ and $\varepsilon_{r,i}$ are the radius and relative permittivity, respectively, for sphere $i$. Substituting Eq. (28) into Eq. (25) and simplifying gives

$$\varepsilon_{r,\text{MG}} = 1+3\frac{\sum_{i=1}^{N} f_i(\varepsilon_{r,i}-1)/(\varepsilon_{r,i}+2)}{1-\sum_{i=1}^{N} f_i(\varepsilon_{r,i}-1)/(\varepsilon_{r,i}+2)}, \tag{29}$$

where $f_i$ is the volume fraction of sphere $i$ within the unit cell. This formula is precisely the Maxwell or, equivalently, Maxwell Garnett, formula for multiphase systems[25] and reduces to Eq. (1) for a two-phase mixture.

The derivation of this result, Eq. (29), is a bit different than that usually employed for the Maxwell Garnett formula. Typically, the derivation of this equation begins with the removal of a spherical region from an infinite and homogeneous dielectric media.[4] In the technique developed here, just the opposite is true. We begin with a large spherical collection of weakly interacting multiphase particles that are immersed in free space. While both approaches yield the same Maxwell Garnet formula, our formula (25) further yields correct $\varepsilon_{r,\text{eff}}$ values including all coupling between spheres.

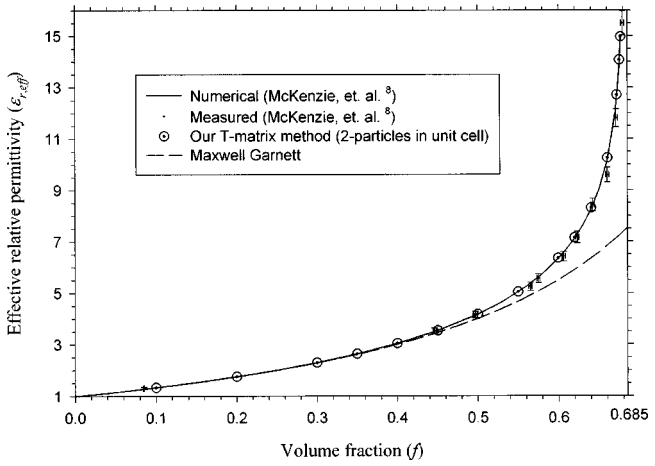


FIG. 3. Computed $\varepsilon_{r,\text{eff}}$ for a body-centered-cubic lattice of conducting spheres. The Maxwell Garnett results are from Eq. (29) and the *T*-matrix results are from Eq. (25) using the solution method described in Sec. II.

## IV. NUMERICAL SOLUTION AND VALIDATION

To provide partial verification of the technique described in Secs. II and III for computing $\varepsilon_{r,\text{eff}}$, comparisons will now be shown with numerical and experimental data presented in the literature.[8] Shown in Fig. 3 is $\varepsilon_{r,\text{eff}}$ computed as a function of the volume fraction $f$ of conducting spheres in a body-centered-cubic (bcc) lattice. The four separate results in Fig. 3 include the Maxwell Garnet results of Eq. (29), our results obtained using Eq. (25) with the *T*-matrix solution of Sec. II as well as accurate numerical and experimental results from the literature.[8] Details of these latter two methods will be discussed separately.

Considering our *T*-matrix results first, $N=2$ conducting spheres were placed within unit cells distributed on a cubic lattice of points. Choosing two spheres provides a partial check of the multiphase capabilities of the code. For the results shown in Fig. 3, a cubic lattice with $J=123$ points was used to truncate the sum $j=1,2,...,J$ in Eq. (18) for a total of 246 conducting spheres, themselves distributed in roughly a spherical region of space. The number of spherical harmonics used in the expansions for the incident potential, Eq. (2), scattered potentials, Eq. (6), and the addition matrix, Eq. (A2), were also truncated as $l=1,2,...,L$ for a total of $L(L+2)$ harmonics.

Depending on the separation of the particles and, consequently, their mutual interaction, the number of harmonics necessary to achieve convergence in $\varepsilon_{r,\text{eff}}$ changes. Shown in Fig. 4 is a plot of the minimum $L$ necessary to achieve less than 1% variation between a convergence tested $\varepsilon_{r,\text{eff}}$ for the bcc lattice of Fig. 3. Only odd $l$ harmonics contribute to $\varepsilon_{r,\text{eff}}$ because of the symmetry of the lattice and the uniform electric field excitation. As is evident in this plot, a very large number of harmonics is necessary to achieve convergence in $\varepsilon_{r,\text{eff}}$ when the particles are nearly touching. In the *T*-matrix numerical computations, we have found that generally single precision computation is sufficient for all but approximately the upper 1%–1.5% of the volume fraction for cubic lattices. For example, double precision computation was necessary only for $f\geqslant 0.67$ in the results of Fig. 3.

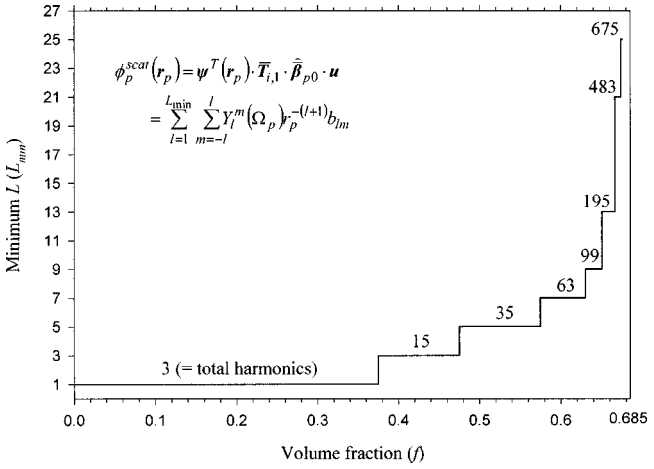


FIG. 4. Minimum $L$ ($L_{\min}$) necessary to achieve less than 1% variation of $\varepsilon_{r,\text{eff}}$ compared with the convergence-tested result for the bcc lattice of Fig. 3. Also shown is the total number of harmonics [$=L_{\min}(L_{\min}+2)$] used in the spherical harmonic expansion for each sphere and the translation matrix $\hat{\boldsymbol{\alpha}}$.

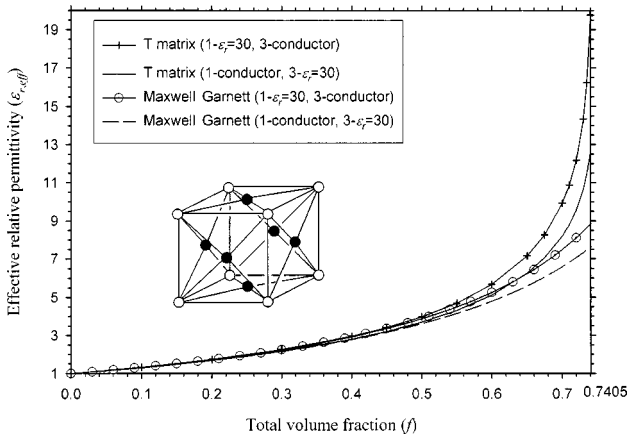


FIG. 5. Effective relative permittivity $\varepsilon_{r,\text{eff}}$ for two different three-phase systems of spheres computed using our $T$-matrix method, Eq. (25), compared with the Maxwell Garnett approximate solution, Eq. (29). The ''1 $-\varepsilon_r=30$, 3-conductor'' has one $\varepsilon_r=30$ sphere at each corner lattice point and three conducting spheres at the three face locations within every unit cell. Conversely, the ''1-conductor, $3-\varepsilon_r=30$'' case has one conducting sphere at each corner lattice point and three spheres with $\varepsilon_r=30$ at the face lattice points.

Our results in Fig. 3 compare extremely well with those of McKenzie *et al.*[8] In that work, the authors present accurate numerical results for the effective permittivity of a cubic lattice of conducting spheres. Their ''method 2'' uses an addition theorem for spherical harmonics, as does our technique use Eq. (31), and is presumably numerically exact. At most, there was less than 0.4% change between our bcc results in Fig. 3 and those of McKenzie *et al.* Furthermore, this difference occurred only when $f \gtrsim 0.67$ and the spheres were nearly touching. Otherwise, the agreement in $\varepsilon_{r,\text{eff}}$ was two decimal places or better. The extremely close agreement in Fig. 3 partially confirms the accuracy of our multiphase formulation and numerical solution.

While there are a number of similarities between the $T$-matrix solution of Sec. II and the technique of McKenzie *et al.*,[8] there are a number of differences which we will elucidate here. First, we have developed a multiphase solution and use the compact and efficient matrix-vector notation of Chew.[17,19] Second, our $T$-matrix solution in Sec. II is directly applicable to any lattice without modification. Last, the $\varepsilon_{r,\text{eff}}$ algorithm in Sec. III is simple, accurate and direct.

Experimental measurements for a bcc lattice of spheres were also presented by McKenzie *et al.*[8] and are shown in Fig. 3. Their effective conductivity measurements were performed on a lattice with nearly perfectly conducting spheres—which is directly analogous at zero frequency to $\varepsilon_{r,\text{eff}}$ for conducting spheres—and are fully described elsewhere.[8] The error bars indicate the measurement error over at least 16 measurements for both the effective conductivity as well as the volume fraction.

Finally, additional comparisons of $\varepsilon_{r,\text{eff}}$ using our $T$-matrix solution with face-centered-cubic (fcc) results [8] and simple cubic (sc) results[7] were also performed. Similarly excellent agreement was observed for all volume fractions, although the results are not shown here.[26] [Equation (11) in that work [26] is incorrect and should be replaced with Eq. (14) in this article. Nevertheless, the final solution and the results there[26] are correct.]

## V. RESULTS

Two examples will now be considered. These examples will both illustrate the usefulness of the multiphase effective permittivity solution presented earlier in this article and demonstrate some interesting behavior that has been observed. The first example is a three-phase system of dielectric and conducting spheres in a fcc lattice. The second is a cubic lattice with unit cells containing a sc cluster of eight conducting spheres.

Regarding the first example, the three-phase fcc lattice is sketched in Fig. 5. All of the spheres in the lattice are the same size, but the corner sphere and the three face spheres within every unit cell are assumed to be of different compositions. Two different cases will be examined for this lattice. In the first case, the corner sphere is assumed to be a conductor and the three face spheres have $\varepsilon_r=30$. Conversely in the second case, the corner sphere has $\varepsilon_r=30$ and the three face spheres are all conductors. The Maxwell Garnett and our $T$-matrix $\varepsilon_{r,\text{eff}}$ results for these two cases are shown in Fig. 5. At low total volume fraction ($f \leqslant 0.3$), the predicted $\varepsilon_{r,\text{eff}}$ is nearly identical regardless of the location of the spheres. This occurs because there is little mutual coupling between the particles (since the MG results are nearly the same as the $T$-matrix results) and both species of spheres have ''large'' relative permittivity.

Beyond $f=0.3$, however, the four curves diverge considerably. In the first case with one conducting particle in a unit cell, it is seen from Fig. 5 that $\varepsilon_{r,\text{eff}}$ is finite (with a value near 12.7) as the spheres approach the touching condition when $f \approx 0.7405$. In the second case with one dielectric sphere per unit cell, $\varepsilon_{r,\text{eff}}$ is becoming very large as the spheres touch. Ideally, $\varepsilon_{r,\text{eff}}$ is becoming singular because in this case the conducting spheres touch. In the first case it was the dielectric spheres that touch and, consequently, $\varepsilon_{r,\text{eff}}$ did not tend towards infinity.

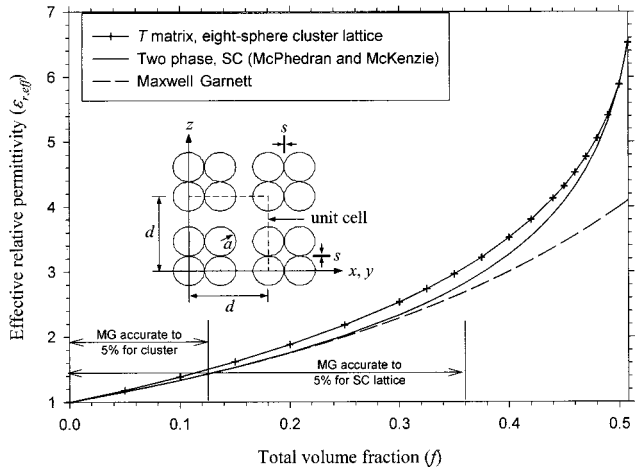


FIG. 6. Effective relative permittivity $\varepsilon_{r,\text{eff}}$ for a nine-phase lattice of clustered conducting spheres computed using our $T$-matrix method, Eq. (25), compared with the two-phase simple cubic solution (Ref. 7) and the Maxwell Garnett approximate solution, Eq. (29). ($s/d=0.005$.)

The second multiphase system we will consider is a cluster of eight identical conducting spheres within unit cells distributed on a cubic lattice, as shown in Fig. 6. The eight spheres are located within the unit cells at the centroids listed in Table II relative to the lattice points. The radius $a$ of the spheres was adjusted to vary the total volume fractions $f$ in the results of Fig. 6. However, the separation distance $s$ between adjacent spheres was held constant.

There are three sets of data shown in Fig. 6. Our $T$-matrix results for $\varepsilon_{r,\text{eff}}$ using Eq. (25) is given along with the Maxwell Garnett solution for this cluster example. Also shown is $\varepsilon_{r,\text{eff}}$ accurately computed for a two-phase simple cubic lattice of conducting spheres.[7] In the results of Fig. 6, $s/d=0.005$ ($d=$unit cell dimension) so that significant mutual interaction between the cluster of spheres would be expected for all volume fractions. However, for small $f(<0.05)$ there is little polarization of the spheres and, consequently, there is also little deviation in $\varepsilon_{r,\text{eff}}$ from the MG predictions.

For $f>0.05$, $\varepsilon_{r,\text{eff}}$ in Fig. 6 varies considerably from the MG results. As shown in Fig. 6, the MG equation predicts ''accurate'' values (within 5%) for $\varepsilon_{r,\text{eff}}$ in this cluster lattice for $f<0.125$. This is in stark contrast to the typical two-phase cubic lattice where MG is accurate up to approximately $f=0.4$. (In Fig. 6, MG is accurate to within 5% for the sc lattice for $f<0.36$.) Of course, the reason that the MG formula fails to predict $\varepsilon_{r,\text{eff}}$ any better in the cluster lattice is because of the mutual interaction of the eight spheres in the cluster. In fact, even within the range of small volume fraction $0.03\lesssim f\lesssim 0.08$, 15 harmonics ($L=3$) were required for a 1% converged $\varepsilon_{r,\text{eff}}$. Of course, more harmonics were required for $f$ larger than this.

TABLE II. Centroid locations for the eight spheres (relative to the lattice points) in the lattice of sphere clusters in Fig. 6. All spheres have radius $a$ and neighboring spheres are separated by distance $s$.

| $i=$particle No. | $x_i$ | $y_i$ | $z_i$ |
|---|---|---|---|
| 1 | 0 | 0 | 0 |
| 2 | $2a+s$ | 0 | 0 |
| 3 | 0 | 0 | $2a+s$ |
| 4 | $2a+s$ | 0 | $2a+s$ |
| 5 | 0 | $2a+s$ | 0 |
| 6 | $2a+s$ | $2a+s$ | 0 |
| 7 | 0 | $2a+s$ | $2a+s$ |
| 8 | $2a+s$ | $2a+s$ | $2a+s$ |

At large volume fraction when $f\gtrsim 0.48$, the $T$-matrix clustered lattice solution and the two-phase sc results are nearly identical. This is expected since in the limit of touching spheres the lattice is approaching the two-phase sc lattice and the ''clustering'' of spheres disappears. However, in the results of Fig. 6 the radius $a$ of the conducting spheres was allowed to increase only to the point where the distance $s$ was maintained between all adjacent spheres. Consequently, the conducting spheres never touch and the effective permittivity $\varepsilon_{r,\text{eff}}$ remains finite.

There is an interesting interpretation of the cluster lattice data in Fig. 6 that we will discuss before concluding. The mutual interaction of the clustered spheres in this lattice causes a ''permittivity enhancement,'' in the words of Doyle and Jacobs.[18] These researchers also predicted such behavior for random collections of spheres. One interpretation of the results in Fig. 6 is that the lattice of clustered spheres behaves as a material type lying somewhere in between purely random materials and those of the typical two-phase lattice. That is, the ''clustered lattice material'' possesses permittivity enhancement at low volume fractions, like the random material, due to clusters of particles but is still, nevertheless, a crystalline material. While interesting in its own right, this clustered lattice material concept is mentioned since it might be possible to apply it—through the use of a suitable Monte Carlo algorithm—to the study of the effective permittivity for purely random materials.

## VI. CONCLUSIONS

A technique to compute the effective permittivity $\varepsilon_{r,\text{eff}}$ of a multiphase lattice containing dielectric and/or conducting spheres was presented in this article. The solution is valid for static fields and approximately true at low frequencies.

This work is unique in several respects. First is the $T$-matrix solution in Sec. II. It applies to lattices with unit cells containing perhaps many different types of dielectric and/or conducting spheres. This multiphase $T$-matrix solution has been presented in the efficient matrix-vector notation of Chew[17] and is an improvement over the notation of previous two-phase solutions.[5,7,8] This work is also unique in that a succinct and accurate equation for the effective permittivity of this multiphase lattice has been presented in Sec. III. When coupled with the multiphase $T$-matrix solution in Sec. II, this new equation for $\varepsilon_{r,\text{eff}}$, Eq. (25), gives a ''numerically exact'' solution and implicitly includes the effects of all mutual interactions between the spheres in the lattice.

Two sets of multiphase results were presented to illustrate the versatility of this technique. In the first set, a cermet

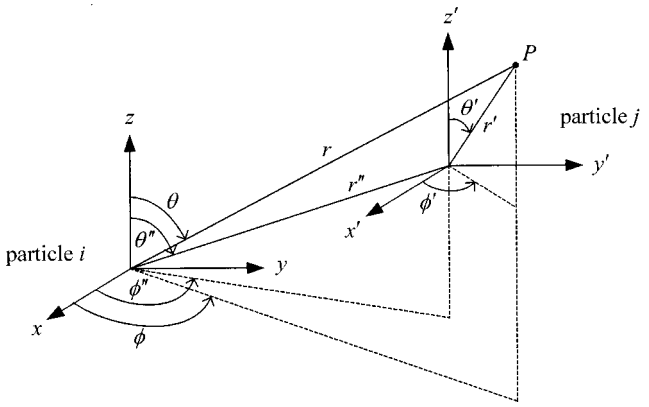


FIG. 7. Coordinate systems used in the application of addition formulas for the translation of spherical harmonics from the coordinate system of particle $i$ to the coordinate system of particle $j$.

composite formed from dielectric and conducting spheres was analyzed. The second multiphase lattice was composed of a cluster of conducting spheres. It was observed that this clustered lattice material exhibited behavior in between that of random materials and monodisperse lattices due to the mutual coupling between the clustered particles.

## APPENDIX

In matrix-vector notation, the two addition (translation) formulas used in this paper are[17]

$$Rg\boldsymbol{\psi}^T(\mathbf{r}_i) = Rg\boldsymbol{\psi}^T(\mathbf{r}_j)\cdot\hat{\hat{\boldsymbol{\beta}}}_{ji} \quad \forall(\mathbf{r}_i,\mathbf{r}_j), \tag{A1}$$

$$\boldsymbol{\psi}^T(\mathbf{r}_i) = Rg\boldsymbol{\psi}^T(\mathbf{r}_j)\cdot\hat{\hat{\boldsymbol{\alpha}}}_{ji} \quad |\mathbf{r}_j| < d_{ij}, \tag{A2}$$

where $d_{ij}$ is the distance between the coordinate system origins of particles $i$ and $j$. (Note that $i$ and $j$ subscripts refer here to two particle numbers rather than the other definitions used in Sec. II.) The function $Rg\boldsymbol{\psi}^T(\mathbf{r}_i)$ was defined in Eq. (5) while $\boldsymbol{\psi}^T(\mathbf{r}_i)$ was defined in Eq. (7). The purpose of this Appendix is to provide expressions for the elements of the matrices $\hat{\hat{\boldsymbol{\alpha}}}_{ji}$ and $\hat{\hat{\boldsymbol{\beta}}}_{ji}$ for static fields in three space.

The method we will use to derive these addition formulas begins with the addition formulas for time-harmonic fields in three-space as provided by Chew.[17] Following the suggestion of Danos and Maximon,[23] the static formulas can be obtained by taking the appropriate low-frequency limits of these time-harmonic equations. A brief derivation of the $\hat{\hat{\boldsymbol{\beta}}}_{ji}$ elements will be shown first followed by the elements of $\hat{\hat{\boldsymbol{\alpha}}}_{ji}$ provided without derivation.

From Eq. (D.14) of Chew,[17] using the coordinate systems in Fig. 7, for all $r$, $r'$ and $r''$

$$Y_l^m(\theta,\phi)j_l(kr) = \sum_{l'=0}^{\infty}\sum_{m'=-l'}^{l'} Y_{l'}^{m'}(\theta',\phi')j_{l'}(kr')\beta_{l'm',lm}. \tag{A3}$$

The unprimed coordinate system is the local spherical coordinate system of particle $i$ while the primed coordinate system is the local spherical coordinate system of particle $j$. To achieve a relationship of the form $Y_l^m(\theta,\phi)r^l$ from Eq. (A3) as $k\to 0$, Eq. (A3) will be multiplied by $k^{-l}$,

$$Y_l^m(\theta,\phi)k^{-l}j_l(kr) = \sum_{l'=0}^{\infty}\sum_{m'=-l'}^{l'} Y_{l'}^{m'}(\theta',\phi') \times j_{l'}(kr')k^{-l}\beta_{l'm',lm}. \tag{A4}$$

Using Eq. (D.15a) of Chew,[17] then

$$\begin{aligned} k^{-l}\beta_{l'm',lm} = \sum_{l''} & 4\pi(-j)^{(l'+l''-l)} \\ & \times Y_{l''}^{m-m'}(\theta'',\phi'')k^{-l}j_{l''}(kr'') \\ & \times(-1)^m\sqrt{(2l+1)(2l'+1)(2l''+1)/(4\pi)} \\ & \times\begin{pmatrix} l & l' & l'' \\ 0 & 0 & 0 \end{pmatrix}\begin{pmatrix} l & l' & l'' \\ -m & m' & m-m' \end{pmatrix}, \end{aligned} \tag{A5}$$

when $l+l'\geq l''\geq|l-l'|$. The last two functions represent the Wigner $3j$ symbols, which are related to the Clebsch–Gordon coefficients through Eq. (D.10) of Chew.[17]

Considering the factor $j_{l''}(kr'')$ in Eq. (A5) and the small argument form

$$j_n(z)\approx\frac{z^n}{(2n+1)!!} \tag{A6}$$

from Eq. (10.1.2) of Abramowitz and Stegun,[27] the summation in Eq. (A5) will be dominated by the term $l''$ that gives the largest value to $(kr'')^{l''}$. This special value of $l''$ will then be the smallest value in the range $l+l'\geq l''\geq|l-l'|$. Therefore, $l''_{\min}=l-l'$ for $l\geq l'$. Substituting this result into Eq. (A5), making use of Eq. (A6) twice more in Eq. (A4) and simplifying yields from Eq. (A4) that

$$Y_l^m(\theta,\phi)r^l = \sum_{l'=0}^{l}\sum_{m'=-l'}^{l'} Y_{l'}^{m'}(\theta',\phi')(r')^{l'}\hat{\beta}_{l'm',lm} \tag{A7}$$

where

$$\begin{aligned} \hat{\beta}_{l'm',lm} = & 4\pi(-1)^m Y_{l-l'}^{m-m'}(\theta'',\phi'') \\ & \times(r'')^{(l-l')}\frac{(2l+1)!!}{(2l'+1)!!(2l-2l'+1)!!} \\ & \times\sqrt{(2l+1)(2l'+1)(2l-2l'+1)/(4\pi)} \\ & \times\begin{pmatrix} l & l' & l-l' \\ 0 & 0 & 0 \end{pmatrix}\begin{pmatrix} l & l' & l-l' \\ -m & m' & m-m' \end{pmatrix}. \end{aligned} \tag{A8}$$

This result in Eq. (A7) is nothing more than the addition formula, Eq. (A1), expressed in succinct matrix-vector notation.

It can be shown that only single terms make nonzero contributions to each of the summations inherent in the Wigner $3j$ coefficients in Eq. (A8). Taking advantage of this and further tedious simplification yields the final result for $l-l'\geq 0$,

$$\hat{\beta}_{l'm',lm} = Y_{l-l'}^{m-m'}(\theta'',\phi'')(r'')^{(l-l')} \times\sqrt{\frac{4\pi(2l+1)}{(2l'+1)(2l-2l'+1)}}\frac{A_{l'}^{m'}A_{l-l'}^{m-m'}}{A_l^m}, \tag{A9}$$

where, following Greengard,[24]

$$A_l^m \equiv \frac{(-1)^l}{\sqrt{(l-m)!(l+m)!}} \tag{A10}$$

Our addition theorem, Eq. (A7), is directly analogous to the ''third addition theorem'' of Greengard.[24] Consequently, the elements of $\hat{\beta}_{l'm',lm}$ in Eq. (A9) are directly analogous to the terms in Eq. (3.53) of Greengard.[24] Here, however, we are using an efficient matrix-vector notation along with different definitions of $Y_l^m$ and the coordinate system translations.

Finally, the elements of the $\hat{\bar{\boldsymbol{\alpha}}}_{ji}$ matrix in Eq. (A2) can be derived in a manner similar to those for $\hat{\bar{\boldsymbol{\beta}}}_{ji}$ presented above. Using the coordinate systems defined in Fig. 7, Eq. (A2) can be expanded to

$$Y_l^m(\theta,\phi) r^{-(l+1)} = \sum_{l'=0}^{\infty} \sum_{m'=-l'}^{l'} Y_{l'}^{m'}(\theta',\phi')(r')^{l'} \hat{\alpha}_{l'm',lm}, \tag{A11}$$

provided $r' < r''$ where $r'' = d_{ij}$. The result of this derivation is that

$$\hat{\boldsymbol{\alpha}}_{l'm',lm} = (-1)^{(l'+m')} Y_{l+l'}^{m-m'}(\theta'',\phi'')(r'')^{-(l+l'+1)} \times \sqrt{\frac{4\pi(2l+1)}{(2l'+1)(2l+2l'+1)}} \frac{A_l^m A_{l'}^{m'}}{A_{l+l'}^{m-m'}}. \tag{A12}$$

## ACKNOWLEDGMENT

This work was supported by the National Science Foundation through Faculty Early Career Development (CAREER) Award No. ECS-9624486.

[1] J. C. Maxwell, *A Treatise on Electricity and Magnetism*, 3rd ed. (Dover, New York, 1954), Art. 314 and 430.
[2] J. C. M. Garnett, Trans. R. Soc. **CCIII**, 385 (1904).
[3] A. H. Sihvola and J. A. Kong, IEEE Trans. Geosci. Remote Sens. **26**, 420 (1988).
[4] D. E. Aspnes, Am. J. Phys. **50**, 704 (1982).
[5] Lord Rayleigh, Philos. Mag. **34**, 481 (1892).
[6] W. T. Doyle, J. Appl. Phys. **49**, 795 (1978).
[7] R. C. McPhedran and D. R. McKenzie, Proc. R. Soc. London, Ser. A **359**, 45 (1978).
[8] D. R. McKenzie, R. C. McPhedran, and G. H. Derrick, Proc. R. Soc. London, Ser. A **362**, 211 (1978).
[9] M. M. Z. Kharadly and W. Jackson, Proc. IEE **100**, 199 (1953).
[10] R. E. Meredith and C. W. Tobias, J. Appl. Phys. **31**, 1270 (1960).
[11] W. M. Merrill, R. E. Diaz, M. M. LoRe, M. C. Squires, and N. G. Alexopoulos, IEEE Trans. Antennas Propag. **47**, 142 (1999).
[12] T. Zakri, J.-P. Laurent, and M. Vauclin, J. Phys. D: Appl. Phys. **31**, 1589 (1998).
[13] A. Kraszewski, J. Microwave Power **13**, 294 (1978).
[14] C. Kittel, *Introduction to Solid State Physics*, 7th ed. (Wiley, New York, 1996), Chaps. 1 and 13.
[15] P. Lalanne, Appl. Opt. **35**, 5369 (1996).
[16] G. Guida, D. Maystre, G. Tayeb, and P. Vincent, J. Opt. Soc. Am. B **15**, 2308 (1998).
[17] W. C. Chew, *Waves and Fields in Inhomogeneous Media* (Van Nostrand Reinhold, New York, 1990).
[18] W. T. Doyle and I. S. Jacobs, Phys. Rev. B **42**, 9319 (1990).
[19] W. C. Chew, J. A. Friedrich, and R. Geiger, IEEE Trans. Geosci. Remote Sens. **28**, 207 (1990).
[20] J. D. Jackson, *Classical Electrodynamics*, 3rd ed. (Wiley, New York, 1999).
[21] J. A. Stratton, *Electromagnetic Theory* (McGraw–Hill, New York, 1941).
[22] S. Stein, Quarterly Appl. Math. **XIX**, 15 (1961).
[23] M. Danos and L. C. Maximon, J. Math. Phys. **6**, 766 (1965).
[24] L. F. Greengard, *The Rapid Evaluation of Potential Fields in Particle Systems* (MIT Press, Cambridge, MA, 1988).
[25] A. Sihvola, A review of dielectric mixing models, Helsinki University of Technology, Report No. 248 (1997).
[26] K. W. Whites, *Proceedings of IEEE Southeastcon '99, Lexington, KY, 1999* (IEEE, Piscataway, NJ, 1999), pp. 249–252.
[27] *Handbook of Mathematical Functions*, edited by M. Abramowitz and I. A. Stegun (US Government Printing Office, Washington, DC, 1964).